Jurnal Ilmiah Farmako Bahari
Journal Homepage : https://journal.uniga.ac.id/index.php/JFB

In Silico Evaluation of Chitosan's Antibacterial Potential Against Gram-Positive and Gram-Negative Bacteria

Selvira Anandia Intan Maulidya[1*], Susi Rahayu[2], Lina Permatasari[1], Hudaynu Patya Putri[1], A'yuni Guban Juniarza[1]

[1]Department of Pharmacy, Faculty of Medicine and Health Sciences, University of Mataram, Jl. Majapahit No. 62, Gomong, Kec. Selaparang, Kota Mataram, Nusa Tenggara Barat, 83125, Indonesia
[2]Department of Physics, Faculty of Mathematics and Natural Sciences, University of Mataram, Jl. Majapahit No. 62, Gomong, Kec. Selaparang, Kota Mataram, Nusa Tenggara Barat, 83125, Indonesia

*Corresponding author: Selvira Anandia Intan Maulidya (selvira@staff.unram.ac.id)

ARTICLE HISTORY

Received: 24 October 2025 | Revised: 17 December 2025 | Accepted: 8 January 2026

Abstract

Chitosan, a natural biopolymer, has attracted attention for its potential antibacterial properties against a wide range of pathogens. The escalating crisis of antibiotic resistance necessitates the exploration of novel antibacterial agents effective against both Gram-positive and Gram-negative bacteria. This study aimed to predict the antibacterial potential of chitosan against *Staphylococcus aureus* (a Gram-positive bacterium) and *Escherichia coli* (a Gram-negative bacterium) using a comprehensive in silico approach. Short chitosan oligomers, specifically trimers, were used to ensure computational feasibility and reliable molecular docking, as full-length polymers are too large for standard docking algorithms. Molecular docking simulations were performed using AutoDock to investigate the interactions between 13 chitosan compounds and the essential bacterial protein DNA gyrase, a key enzyme involved in DNA replication and repair. Binding affinities, interaction patterns (such as hydrogen bonding and hydrophobic contacts), and conformational changes were analyzed. The ligand showing the most favorable docking profile was further evaluated via molecular dynamics simulations using OpenMMDL to assess the stability of the complex over time. The results indicated that the chitosan derivatives, namely aminoethyl chitosan and dimethylaminoethyl chitosan, interact favorably with DNA gyrase in *S. aureus* and *E. coli*, respectively, with differential binding energies and interaction modes suggesting potential variations in inhibitory mechanisms between Gram-positive and Gram-negative bacteria. These computational findings support the potential of chitosan as a broad-spectrum antibacterial agent and provide a theoretical framework to guide further in vitro and in vivo validation of chitosan as a novel antibacterial compound.

Keywords: antibiotic, biopolymer, molecular docking, molecular dynamics

Introduction

The escalating global crisis of antibiotic resistance poses a significant threat to public health, with multidrug-resistant (MDR) pathogens increasingly challenging conventional treatment regimens.[1] This situation underscores the urgent need for the discovery and development of novel antimicrobial agents, particularly those possessing

ISSN: 2087-0337
E-ISSN: 2715-9949

broad-spectrum activity against both Gram-positive and Gram-negative bacteria. These two major bacterial groups exhibit fundamental differences in their cell wall structures; specifically, Gram-positive bacteria dictate their susceptibility to various antimicrobial compounds.[2]

In the quest for alternative antimicrobials, natural biopolymers have garnered considerable attention due to their biocompatibility, biodegradability, and inherent biological activities. Among these, chitosan, a natural amino polysaccharide derived from chitin, has emerged as a promising candidate. Chitosan is widely recognized as an effective antibacterial agent due to its potent antimicrobial properties.[3–5] The proposed mechanisms for chitosan's antibacterial action are diverse, encompassing disruption of bacterial cell membranes, chelation of essential metal ions, binding to DNA to inhibit mRNA synthesis, and interaction with essential microbial proteins.[6] Chitosan's antibacterial activity is affected by a range of intrinsic and extrinsic factors, such as pH, concentration, bacterial strain, source of chitosan, degree of polymerization, and other related parameters.[7]

Despite the growing body of evidence supporting chitosan's antimicrobial potential, a detailed understanding of its molecular interactions with specific bacterial targets, particularly distinguishing its efficacy and mechanisms against Gram-positive versus Gram-negative strains, remains an area of active investigation. The structural and physicochemical properties of chitosan, such as its molecular weight and degree of deacetylation, are known to influence its biological activity.[8,9] Elucidating these structure-activity relationships at a molecular level is crucial for optimizing chitosan-based antimicrobial therapies.

Computational, or *in silico*, approaches offer a powerful, robust, cost-effective, and time-efficient platform for predicting and analyzing biomolecular interactions.[10] Techniques such as molecular docking can simulate the binding of a ligand, such as chitosan oligomers—in this study, specifically chitosan trimers—to a receptor, such as essential bacterial proteins, providing insights into binding affinities, interaction modes, and potential inhibitory mechanisms.[11] Using short oligomers like trimers ensures computational feasibility while retaining key structural features relevant for binding. Such predictive studies can significantly narrow down experimental efforts and guide the rational design of more potent antimicrobial derivatives.

Therefore, this study aims to employ an *in silico* approach to predict and compare the antibacterial activity of chitosan against selected Gram-positive and Gram-negative bacterial strains. By investigating the molecular interactions between chitosan and key essential protein targets within these distinct bacterial groups, we seek to elucidate potential mechanisms of action and provide a computational basis for its broad-spectrum antibacterial efficacy. The findings from this research are anticipated to contribute to a deeper understanding of chitosan's antimicrobial properties and support its further development as a viable alternative or adjunct to conventional antibiotics.

ISSN: 2087-0337
E-ISSN: 2715-9949

Method

Equipment

The hardware used for molecular docking was a 14-inch HP with an Intel(R) Core(TM) i3-6006U processor, 12 GB of RAM, a CPU speed of 2.00 GHz, and a 256GB SSD. MarvinSketch was used to draw chemical structures. The docking simulations were carried out using AutoDock Tools v1.5.6, developed by the Center for Computational Structural Biology (USA), and BIOVIA Discovery Studio Visualizer 2025, created by Dassault Systèmes. Molecular dynamics testing was conducted using the OpenMMDL software (Germany). Additionally, SwissADME (Swiss Institute of Bioinformatics) was employed to evaluate the drug-likeness of the compounds based on Lipinski's Rule of Five and ADMET (absorption, distribution, metabolism, excretion, and toxicity) properties. At the same time, ProTox 3.0 (Germany) was used to predict their toxicity profiles.

Material

The target receptor, DNA gyrase crystal structures for *S. aureus* (PDB ID: 4P8O) and. *E. coli* (PDB ID: 4ZVI) were obtained from the Protein Data Bank. 13 compounds of chitosan and its derivatives structures were collected from PubChem.

Procedure

Geometrical Optimization

The 3D molecular structures of chitosan and its derivatives were modeled and geometrically optimized using MarvinSketch. The resulting optimized structures were then exported in PDB format using OpenBabel software.

Receptor Preparation

Receptor preparation involved downloading the DNA gyrase structures of *S. aureus* (PDB ID: 4P8O) and *E. coli* (PDB ID: 4ZVI) from the RCSB Protein Data Bank (https://rcsb.org) in PDB format. The selection of receptor target structures was based on criteria such as high-resolution crystallographic data and the presence of a co-crystallized inhibitor, considered the native ligand. The receptor structures were refined through a cleaning process to improve their quality and accuracy, which involved removing all bound ligands and water molecules. Subsequently, polar hydrogen atoms were added, and Kollman charges were applied using AutoDock Tools v1.5.6.[10]

Molecular Docking

The docking protocol was validated by re-docking the native ligand into the active site of the bacterial DNA gyrase receptor. Molecular docking was performed using previously validated parameters and the Lamarckian Genetic Algorithm (LGA). A grid box was centered on the active site of the receptor with dimensions of 40 x 40 x 40 Å and a grid spacing of 0.375 Å, covering all key catalytic residues. Subsequently, the optimized three-dimensional structures of chitosan derivatives were docked into the active site of bacterial DNA gyrase. The docking results were evaluated based on binding free energy (ΔG), inhibition constants (Ki), and binding conformations. The ligand exhibiting the most favorable docking performance was selected for further analysis using molecular dynamics (MD) simulation.

ISSN: 2087-0337
E-ISSN: 2715-9949

Molecular Dynamic Simulations

Molecular dynamics simulations were performed using the OpenMMDL pipeline. The protein–ligand complex was prepared and parameterized using the appropriate force fields. The system was solvated in an explicit water box and neutralized with counterions. Energy minimization was performed to eliminate steric clashes, followed by equilibration under NVT and NPT conditions. The production molecular dynamics simulation was then run for 30 ns at constant temperature and pressure. Trajectory data were collected for further structural and interaction analysis.

ADMET and Toxicity Profiling of Ligands

Access SwissADME at http://www.swissadme.ch, then enter a list of ligands in canonical SMILES format. SwissADME was employed to evaluate drug-likeness based on Lipinski's Rule of Five and to predict pharmacokinetic properties, including absorption, distribution, metabolism, excretion, and toxicity (ADMET). Ligand toxicity was further assessed using ProTox 3.0 (https://tox.charite.de/protox3/), which provides predicted LD50 values, toxicity classes, and potential organ toxicity. The combined analysis enabled the identification of compounds with favorable drug-likeness, pharmacokinetic profiles, and low predicted toxicity, which were subsequently used for molecular docking and molecular dynamics simulations.

Result

Table 1. Results of Molecular Docking Validation

PDB ID	*Grid Box*			RMSD (Å)	*Binding affinity* (kcal/mol)
	X	Y	Z		
4P8O	49.582	-5.015	19.291	0.52	-9.17
4ZVI	-12.638	20.712	21.240	1.816	-10.10

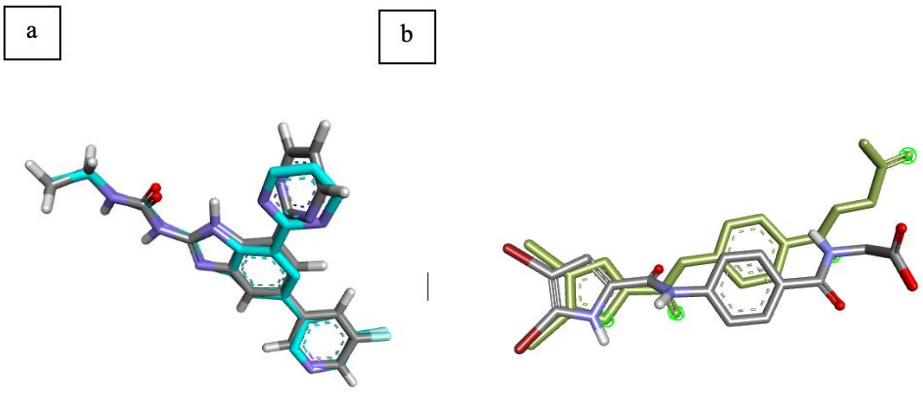

Figure 1. Validation method of molecular interaction between ligand and receptor target (a) *S. aureus* DNA gyrase (4P8O) (b) *E. coli* DNA gyrase (4ZVI)

ISSN: 2087-0337
E-ISSN: 2715-9949

Table 2. Docking Results for *S. Aureus* DNA Gyrase

No.	Ligand	Binding Free Energy (Kcal/mol)	Inhibition Constant (Ki)
1	Chitosan	-1.04	172.69 mM
2	Carboxymethyl Chitosan	-5.90	47.21 uM
3	Glycol Chitosan	+6.92	-
4	Aminoethyl chitosan	-6.67	12.84 uM
5	Dimethylaminoethyl Chitosan	-3.43	3.88 mM
6	Diethylaminoethyl Chitosan	-0.90	220.20 mM
7	N-Succinyl Chitosan	-2.31	20.31 mM
8	Chitosan trifluoroacetate	-2.39	17.76 mM
9	Chitosan malate	+0.49	-
10	Cinnamyl-Chitosan	0.96	197.88 mM
11	Hydroxybutyl-Chitosan	-1.37	99.22 mM
12	O-hydroxyethylchitosan	-5.39	111.11 uM
13	Amino-chitosan	-4.82	295.17 uM
14	Native Ligand	-9.17	188.37 nM

Table 3. Docking Results for *E. Coli* DNA Gyrase

No.	Ligand	Binding Free Energy (Kcal/mol)	Inhibition Constant (Ki)
1	Chitosan	-5.81	55.34 mM
2	Carboxymethyl Chitosan	-5,29	132.99 uM
3	Glycol Chitosan	-3,25	4.14 mM
4	Aminoethyl chitosan	-5.43	105.36 uM
5	Dimethylaminoethyl Chitosan	-6.95	8.07 uM
6	Diethylaminoethyl Chitosan	-6,56	15.43 uM
7	N-Succinyl Chitosan	-5,68	68.57 uM
8	Chitosan trifluoroacetate	-3,91	1.37 mM
9	Chitosan malate	-2,61	12.26 mM
10	Cinnamyl-Chitosan	-6,4	20.24 uM
11	Hydroxybutyl-Chitosan	-2,41	17.02 mM
12	O-hydroxyethylchitosan	-3,38	3.33 mM
13	Amino-chitosan	-5,88	49.16 uM
14	Native Ligand	-10.10	39.62 nM

ISSN: 2087-0337
E-ISSN: 2715-9949

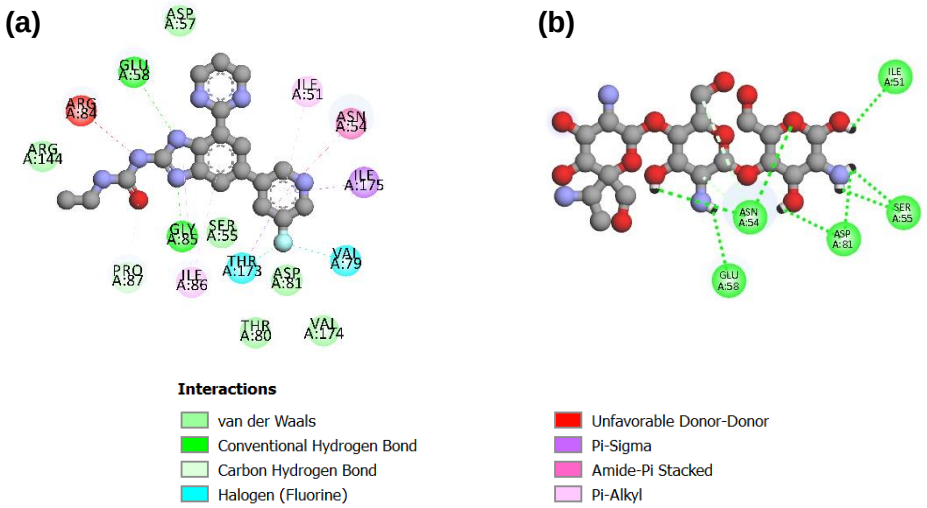

Figure 2. Two-dimensional interactions between amino acid residues of *Staphylococcus aureus* DNA gyrase and the (a) native ligand, (b) aminoethyl chitosan

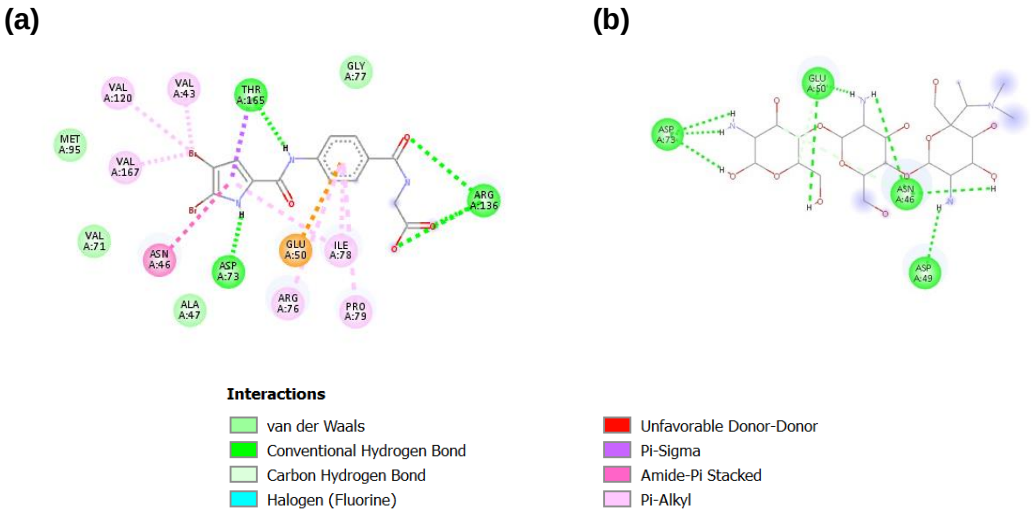

Figure 3. Two-dimensional interactions between amino acid residues of *E. coli* DNA gyrase and the (a) native ligand, (b) dimethylaminoethyl chitosan

ISSN: 2087-0337
E-ISSN: 2715-9949

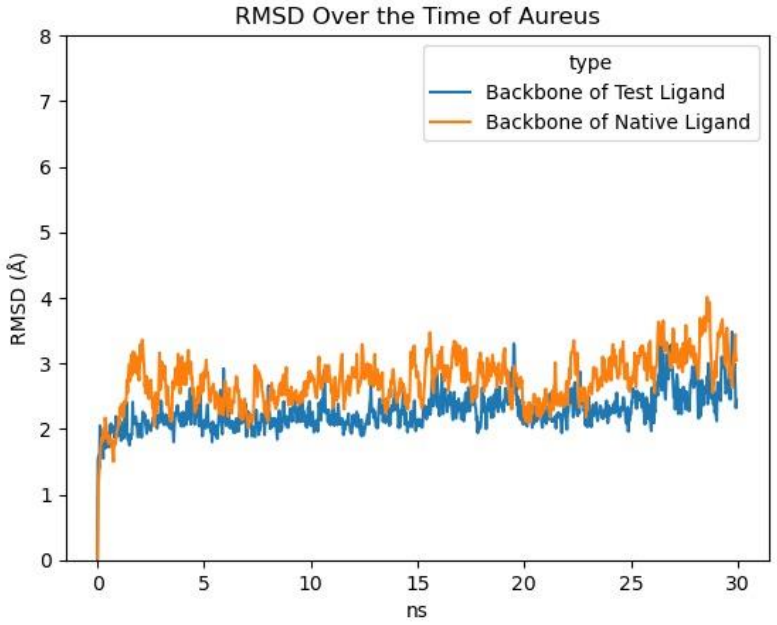

Figure 4. RMSD plot of the protein backbone for the *S. aureus* DNA gyrase complexes with aminoethyl chitosan (blue) and the native ligand (orange)

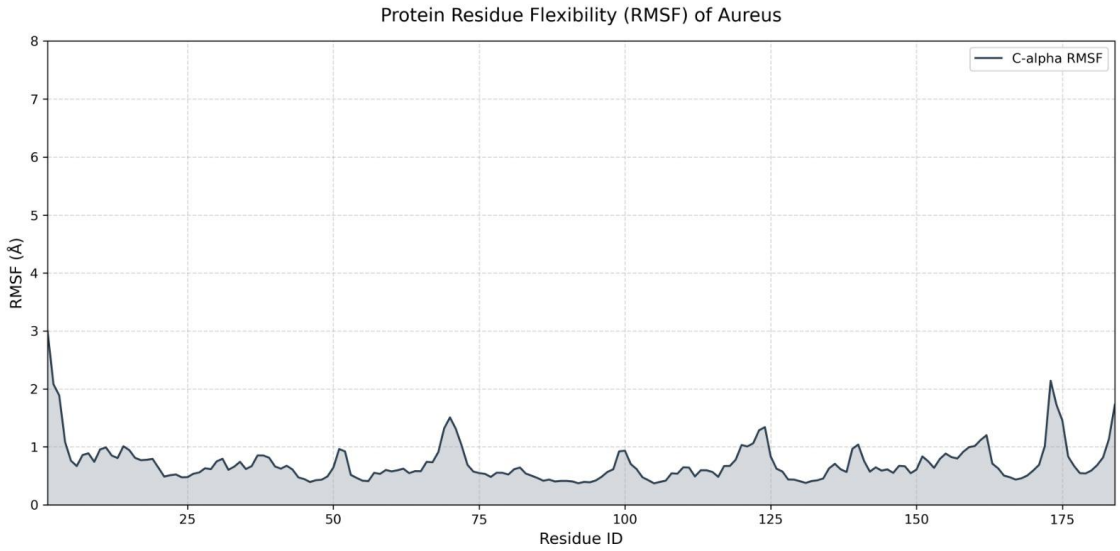

Figure 5. RMSF plot of the protein backbone for the *S. aureus* DNA gyrase complexes with aminoethyl chitosan (blue) and the native ligand (orange)

ISSN: 2087-0337
E-ISSN: 2715-9949

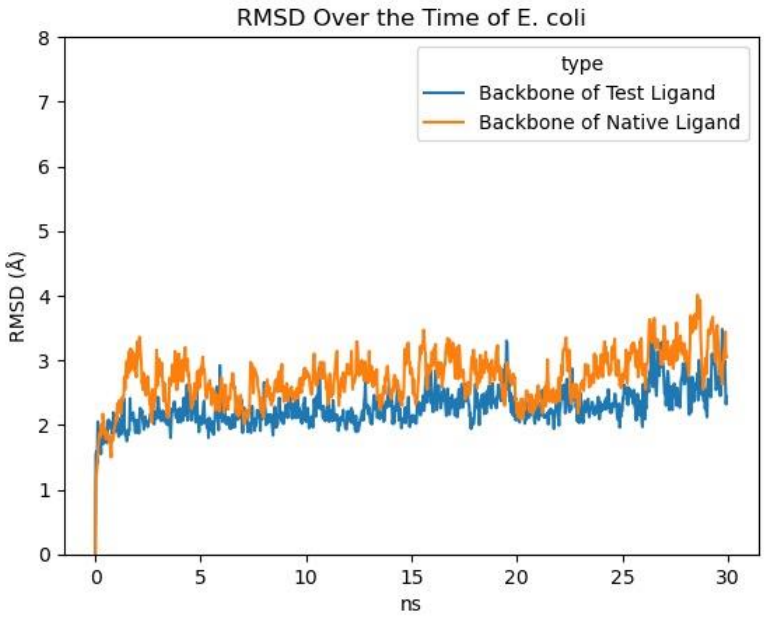

Figure 6. RMSD plot of the protein backbone for the *E. coli* DNA gyrase complexes with dimethylaminoethyl chitosan (blue) and the native ligand (orange)

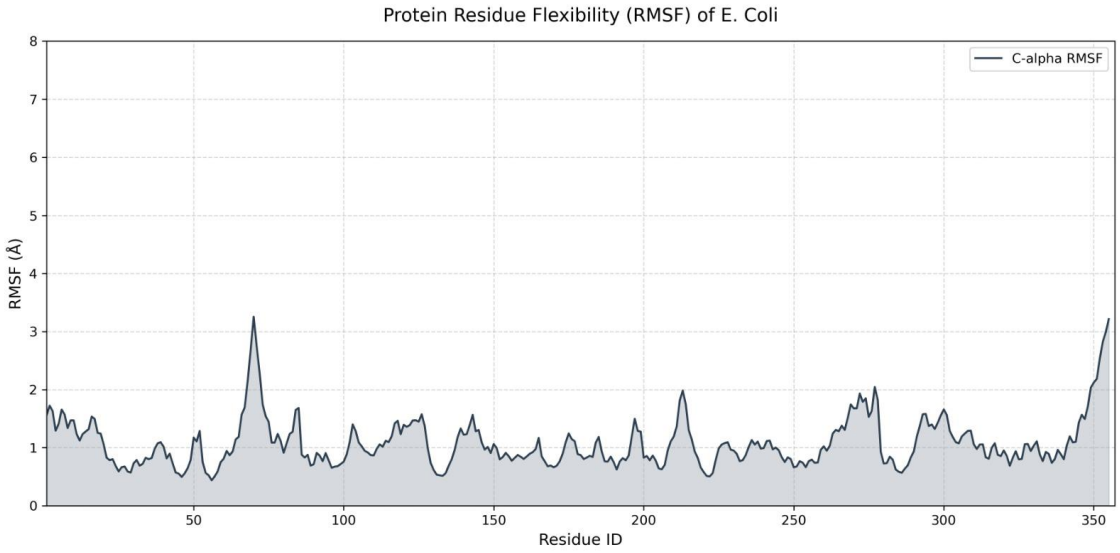

Figure 7. RMSF plot of the protein backbone for the *E. coli* DNA gyrase complexes with dimethylaminoethyl chitosan (blue) and the native ligand (orange)

ISSN: 2087-0337
E-ISSN: 2715-9949

Table 4. Predicted Pharmacokinetic Properties of Chitosan Compounds

No	Derivat Kitosan	GI Absorption	Distribution (Lipophilicity Log P o/w)	Metabolism (Cytochrome metabolism)
1	Chitosan	Low	-4,64	-
2	Carboxymethyl Chitosan	Low	-5,57	-
3	Glycol Chitosan	Low	-5,58	-
4	Aminoethyl chitosan	Low	-5,80	-
5	Dimethylaminoethyl Chitosan	Low	-5,34	-
6	Diethylaminoethyl Chitosan	Low	-5,08	-
7	N-Succinyl Chitosan	Low	-5,28	-
8	Chitosan trifluoroacetate	Low	-4,93	-
9	Chitosan malate	Low	-5,84	-
10	Cinnamyl-chitosan	Low	-3,59	-
11	Hydroxybutyl chitosan	Low	-5,17	-
12	O-hydroxyethylchitosan	Low	-5,42	-
13	Amino-chitosan	Low	-6,44	-

Table 5. Toxicity Prediction of Chitosan Compounds

No	Derivat Kitosan	Hepatotoxicity	Mutagenicity	Carcinogenicity
1	Chitosan	Inactive	Inactive	Inactive
2	Carboxymethyl Chitosan	Inactive	Inactive	Inactive
3	Glycol Chitosan	Inactive	Inactive	Inactive
4	Aminoethyl chitosan	Inactive	Inactive	Inactive
5	Dimethylaminoethyl Chitosan	Inactive	Inactive	Inactive
6	Diethylaminoethyl Chitosan	Inactive	Inactive	Inactive
7	N-Succinyl Chitosan	Inactive	Inactive	Inactive
8	Chitosan trifluoroacetate	Inactive	Inactive	Inactive
9	Chitosan malate	Inactive	Inactive	Inactive
10	Cinnamyl-chitosan	Inactive	Inactive	Inactive
11	Hydroxybutyl chitosan	Inactive	Inactive	Inactive
12	O-hydroxyethylchitosan	Inactive	Inactive	Inactive
13	Amino-chitosan	Inactive	Inactive	Inactive

Table 6. Drug-Likeness Evaluation Based on Lipinski's Rule of Five

No.	Derivat Kitosan	Lipinski's Rule of Five				
		MW (Da)	LogP (MLOGP)	HBD	HBA	Lipinski
1	Chitosan	610.87	-5.47	11	16	No
2	Carboxymethyl Chitosan	543.52	-6.16	11	16	No
3	Glycol Chitosan	649.68	-6.79	11	19	No
4	Aminoethyl chitosan	544.55	-6.42	12	17	No
5	Dimethylaminoethyl Chitosan	572.60	-5.98	11	17	No

ISSN: 2087-0337
E-ISSN: 2715-9949

Table 6. (Extension)

No.	Derivat Kitosan	Lipinski's Rule of Five				
		MW (Da)	LogP (MLOGP)	HBD	HBA	Lipinski
6	Diethylaminoethyl Chitosan	600.66	-5.56	11	17	No
7	N-Succinyl Chitosan	583.54	-5.74	10	17	No
8	Chitosan trifluoroacetate	613.49	-5.74	11	21	No
9	Chitosan malate	761.68	-7.42	14	21	No
10	Cinnamyl-chitosan	617.64	-4.65	11	16	No
11	Hydroxybutyl chitosan	573.59	-5.98	12	17	No
12	O-hydroxyethylchitosan	545.54	-6.02	11	17	No
13	Amino-chitosan	516.50	-6.48	12	17	No

Discussion

Geometrical Optimization

The first step in this study involved optimizing the 3D structures of chitosan and its derivatives. Geometry optimization plays a crucial role in modern computational chemistry, particularly in electronic structure calculations related to chemical properties and reactions. It is essential for identifying the most stable conformation of a ligand's 3D structure and determining its minimum energy.[11] In this research, geometry optimization was performed using the MMFF94 force field.

Molecular Docking

Molecular docking in this study was conducted using AutoDock Tools, a software tool that had been previously validated. Validation of the docking method was assessed based on the Root Mean Square Deviation (RMSD) value, with a threshold of less than 2.0 Å indicating acceptable accuracy. The method met this criterion, as shown in Table 1. Docking validation on both *S. aureus* and *E. coli* DNA gyrase yielded RMSD values of less than 2.

Preparation for docking the 16 selected ligands was performed using AutoDock Tools v1.5.6. The docking procedure, executed in AutoDock, generated predictions of binding free energy (ΔG) and visualizable interaction poses. The ΔG value reflects the binding affinity and stability of the ligand–receptor complex, with lower values indicating stronger and more stable interactions. This molecular docking analysis compared the ΔG values of the 16 compounds to the ΔG value of a reference ligand bound to bacterial DNA gyrase. Tables 2 and 3 present the docking results of chitosan and its derivatives against the bacterial DNA gyrase, with the reference ligand originating from the same receptor. Based on the docking results, none of the chitosan compounds or their derivatives had a lower binding free energy than the native ligand. In the case of *S. aureus* DNA gyrase, it was found that several compounds exhibited positive binding free energy values. In molecular docking studies, the binding free energy (ΔG) serves as an indicator of the thermodynamic favorability of the interaction between a ligand and its target protein. A negative ΔG value implies that the binding process is exergonic, spontaneous, and energetically favorable, suggesting a stable ligand–protein complex formation. Conversely, a positive binding free energy reflects an unfavorable interaction, indicating that the ligand does not bind spontaneously to the target and that the formation of the complex would require an input of energy. Among the chitosan derivative compounds evaluated, aminoethyl chitosan demonstrated the lowest binding free energy

ISSN: 2087-0337
E-ISSN: 2715-9949

upon docking to *S. aureus* DNA gyrase; however, its binding affinity remained inferior to that of the native ligand.

The docking results of chitosan and its derivatives against *E. coli* DNA gyrase indicate that all compounds exhibit antibacterial activity, as evidenced by their negative binding free energy values. However, none of them showed a binding energy lower than that of the native ligand. The lowest binding free energy was observed for dimethylaminoethyl chitosan, with a value of -7.85 kcal/mol. Although the precise mechanism underlying chitosan's antibacterial effects remains incompletely characterized, its antimicrobial activity is widely regarded as multifaceted and influenced by multiple independent factors. The most commonly proposed mechanism involves electrostatic interactions: the polycationic nature of chitosan enables it to bind to the negatively charged bacterial cell surface, compromising membrane integrity and increasing permeability, which ultimately leads to leakage of intracellular components and cell death.[12,13] Additionally, low-molecular-weight chitosan can penetrate bacterial cells and interfere with fundamental processes such as mRNA synthesis, DNA transcription, and protein translation. This docking result is consistent with several other studies, which state that chitosan has bactericidal/bacteriostatic effects against various common bacteria, including both Gram-positive and Gram-negative strains.[14–16]

Aminoethyl chitosan and dimethylaminoethyl chitosan were selected for further analysis. The interaction poses of the two compounds on the active site of the bacterial DNA gyrase were compared, which refers to the ligand reference binding pose. The purpose is to determine which features of the interaction occur at the active site of bacterial DNA gyrase in relation to its antibacterial activity. The results of the 2D visualization of the reference ligand, aminoethyl chitosan, and dimethylaminoethyl chitosan are presented in Figures 2 and 3, respectively. From the visualization, it can be seen that the interaction poses between aminoethyl chitosan and dimethylaminoethyl chitosan exhibit different numbers of interaction profiles. The visualization of the complex between aminoethyl chitosan and *S. aureus* DNA gyrase revealed multiple hydrogen-bond interactions involving Ile51, Ser55, Asp81, Asn54, and Glu58. Meanwhile, the complex of dimethylaminoethyl chitosan with *E. coli* DNA gyrase exhibited hydrogen-bond interactions with four amino acid residues: Asp73, Asp49, Asn46, and Glu50. The chitosan interacted with key active-site residues also involved in native ligand binding, although through different interaction types.

Molecular Dynamic Simulation

Molecular dynamics (MD) simulations estimate the movements of every atom in a protein or other molecular system over time by applying a general physical model of how atoms interact. These simulations are capable of capturing a wide range of crucial biomolecular processes, such as conformational changes, ligand binding, and protein folding, while providing atomic positions with femtosecond-level temporal resolution. Additionally, MD simulations can predict how biomolecules respond at the atomic scale to various perturbations, including mutations, phosphorylation, protonation, or the addition or removal of ligands.[17,18] The RMSD analysis of the complex between *S. aureus* DNA gyrase backbone and aminoethyl chitosan (Figure 4) showed that both complexes equilibrated within the first few nanoseconds and maintained stable conformations throughout the 30 ns simulation. The aminoethyl chitosan complex displayed RMSD values around 2.0–2.8 Å, while the native ligand complex had slightly higher fluctuations up to 3.5–4.0 Å toward the end of the simulation. Still, neither exhibited signs of significant structural destabilization. Complementary RMSF analysis (Figure 5) revealed that most residues fluctuated below 1.5 Å, indicating overall protein rigidity, with higher flexibility localized at the N-terminus and loop regions near residues 70, 120, and 175–180, typical of solvent-exposed areas. Importantly, binding site residues remained

ISSN: 2087-0337
E-ISSN: 2715-9949

relatively stable, supporting sustained ligand interactions. Together, these findings indicate that both ligand–protein complexes are structurally stable and maintain functional conformations under dynamic conditions, consistent with reliable docking predictions.

The root mean square deviation (RMSD) analysis was employed to assess the overall structural stability of *E. coli* DNA gyrase in complex with dimethylaminoethyl chitosan during the 30 ns molecular dynamics simulation and was compared with the native ligand–bound system (Figure 6). Both complexes exhibit a rapid increase in RMSD during the initial 1–2 ns, corresponding to the equilibration phase in which the protein adapts to the solvated environment and optimizes protein–ligand interactions. Following equilibration, the dimethylaminoethyl chitosan–DNA gyrase complex exhibits a stable RMSD profile, fluctuating narrowly between 2.0 and 2.5 Å throughout the simulation. This relatively low and consistent RMSD indicates that the binding of dimethylaminoethyl chitosan contributes to maintaining the structural integrity of the protein backbone, suggesting a well-stabilized complex.[19] In contrast, the native ligand–DNA gyrase complex shows comparatively higher RMSD values, ranging from approximately 2.3 to 3.5 Å, with increased fluctuations particularly toward the later stages of the simulation. These deviations suggest greater conformational flexibility of the protein backbone and potential rearrangements within the binding region when the protein is bound to its native ligand. Importantly, RMSD values for both systems remain below 4 Å, indicating that no significant structural destabilization or unfolding occurs. Nevertheless, the lower RMSD observed for the dimethylaminoethyl chitosan complex suggests enhanced stability and stronger protein–ligand interactions compared to the native ligand. The root mean square fluctuation (RMSF) analysis was conducted to evaluate the residue-specific flexibility of *E. coli* DNA gyrase in the presence of dimethylaminoethyl chitosan (Figure 7). Overall, the RMSF profile indicates that most residues fluctuate by less than 1.5 Å, suggesting a generally stable protein structure during the simulation. Crucially, residues within the presumed binding region display moderate to low RMSF values, implying that dimethylaminoethyl chitosan binding restricts excessive residue motion and contributes to local stabilization of the active site. This reduced flexibility near the binding interface supports the RMSD findings and indicates that the ligand effectively anchors key protein regions. The relatively low RMSF values across the core regions of DNA gyrase imply that the protein maintains its functional conformation throughout the simulation. The absence of extreme fluctuations further confirms that ligand binding does not induce destabilizing structural perturbations.

ADMET and Drug-Likeness Prediction

Early drug development requires the prediction of absorption, distribution, metabolism, and elimination (ADME) profiles to facilitate the selection of promising candidates before synthesis. Since *in vivo* ADME evaluation is expensive, time-consuming, and ethically challenging, *in silico* approaches offer a faster, safer, and more cost-effective alternative. In this study, SwissADME was employed to predict the ADMET properties of chitosan and its derivatives. The development of effective and safe drugs depends on a balanced interplay between pharmacodynamic activity and favorable pharmacokinetic behavior, including acceptable ADMET characteristics.[20,21] The ADMET prediction and drug-likeness assessment of aminoethyl chitosan and dimethylaminoethyl chitosan provide essential insights into their pharmacokinetic behavior, safety profile, and suitability as drug-related materials. Both derivatives exhibit comparable ADMET characteristics, reflecting their shared chitosan backbone while highlighting the influence of chemical substitution on physicochemical properties. The predicted gastrointestinal (GI) absorption for both aminoethyl chitosan and dimethylaminoethyl chitosan is low, which is consistent with their high molecular weights (544.55 and 572.60 g/mol,

respectively) and pronounced hydrophilicity. Their extremely low lipophilicity values (log P ranging from −5.80 to −6.42 for aminoethyl chitosan and −5.34 to −5.98 for dimethylaminoethyl chitosan) indicate poor membrane permeability, a known limitation for oral bioavailability. Such characteristics are typical of polysaccharide-based polymers, suggesting that neither derivative is well-suited for passive diffusion across biological membranes when administered orally. From a drug-likeness perspective, both compounds markedly violate Lipinski's rule of five, primarily due to their high molecular weights and excessive numbers of hydrogen bond donors (HBDs) and acceptors (HBAs). Aminoethyl chitosan presents 12 HBDs and 17 HBAs, while dimethylaminoethyl chitosan shows a slightly reduced HBD count of 11 with the same number of HBAs. These features contribute to strong intermolecular hydrogen bonding and high aqueous solubility but significantly limit permeability and classical small-molecule drug behavior. Consequently, these chitosan derivatives should not be considered conventional drug candidates but rather functional excipients or carrier systems. Despite their unfavorable drug-likeness metrics, both aminoethyl chitosan and dimethylaminoethyl chitosan demonstrate a favorable safety profile based on in silico toxicity predictions. The absence of predicted hepatotoxicity, carcinogenicity, and mutagenicity suggests low intrinsic toxicity, supporting their potential for biomedical applications.

Conclusion

The *in silico* molecular docking analysis indicates that chitosan derivatives exhibit promising antibacterial activity, with aminoethyl chitosan showing the strongest binding affinity against *Staphylococcus aureus* and dimethylaminoethyl chitosan demonstrating favorable interactions with *Escherichia coli*. These results support their potential as antibacterial agents. However, ADMET and drug-likeness assessments suggest that both derivatives are unsuitable as orally active small-molecule drugs due to low gastrointestinal absorption and unfavorable physicochemical properties. Despite this limitation, their low predicted toxicity, metabolic stability, and high hydrophilicity highlight their promise as drug-delivery carriers, absorption enhancers, or biomaterials, particularly for nanoparticle-based, localized, or parenteral applications. Further experimental studies are required to validate their translational potential.

Acknowledgement

This study was supported by a research grant from LPPM at the University of Mataram under contract no. 2293/UN18.L1/PP/2025, as well as by various collaborators who contributed to the research.

Reference

1. Murray CJ, Ikuta KS, Sharara F, Swetschinski L, Robles Aguilar G, Gray A, et al. Global burden of bacterial antimicrobial resistance in 2019: a systematic analysis. Lancet. 2022;399(10325):629–55.
2. Silhavy TJ, Kahne D, Walker S. The bacterial cell envelope. Cold Spring Harb Perspect Biol. 2010;2(5):1–17.
3. Edo GI, Yousif E, Al-Mashhadani MH. Chitosan: An overview of biological activities, derivatives, properties, and current advancements in biomedical applications. Carbohydr Res. 2024;542.
4. El-Araby A, Janati W, Ullah R, Ercisli S, Errachidi F. Chitosan, chitosan derivatives, and chitosan-based nanocomposites: eco-friendly materials for advanced applications (a review). Front Chem. 2023;11:01–21.
5. Husni P, Junaedi J, Gozali D. Penentuan aktivitas antibakteri kitosan Cilamaya terhadap Staphylococcuss aureus. Farmasains J Ilm Ilmu Kefarmasian. 2024;11(1):36–47.

6. Li J, Zhuang S. Antibacterial activity of chitosan and its derivatives and their interaction mechanism with bacteria: current state and perspectives. Eur Polym J. 2020;138:1–12.
7. Ardean C, Davidescu CM, Nemeş NS, Negrea A, Ciopec M, Duteanu N, et al. Factors influencing the antibacterial activity of chitosan and chitosan modified by functionalization. Int J Mol Sci. 2021;22(14):1–28.
8. Verlee A, Mincke S, Stevens C V. Recent developments in antibacterial and antifungal chitosan and its derivatives. Carbohydr Polym. 2017;164:268–83.
9. Kairys V, Baranauskiene L, Kazlauskiene M, Matulis D, Kazlauskas E. Binding affinity in drug design: experimental and computational techniques. Expert Opin Drug Discov. 2019;14(8):755–68.
10. Morris GM, Huey R, Olson AJ. Using autodock for ligand-receptor docking. Vol. 24, Current Protocols in Bioinformatics. 2008. p. 1–40.
11. Zheng J, Frisch MJ. Efficient geometry minimization and transition structure optimization using interpolated potential energy surfaces and iteratively updated hessians. J Chem Theory Comput. 2017;13(12):6424–32.
12. Yang Y, Gupta VK, Amiri H, Pan J, Aghbashlo M, Tabatabaei M, et al. Recent developments in improving the emulsifying properties of chitosan. Int J Biol Macromol. 2023;239.
13. Yilmaz Atay H. Antibacterial activity of chitosan-based systems. In: Functional Chitosan: Drug Delivery and Biomedical Applications. Springer; 2019. p. 457–89.
14. Shankar S, Rhim JW. Preparation of sulfur nanoparticle-incorporated antimicrobial chitosan films. Food Hydrocoll. 2018;82:116–23.
15. Helander IM, Nurmiaho-Lassila EL, Ahvenainen R, Rhoades J, Roller S. Chitosan disrupts the barrier properties of the outer membrane of Gram-negative bacteria. Int J Food Microbiol. 2001;71(2–3):235–44.
16. Duan C, Meng X, Meng J, Khan MIH, Dai L, Khan A, et al. Chitosan as a preservative for fruits and vegetables: a review on chemistry and antimicrobial properties. J Bioresour Bioprod. 2019;4(1):11–21.
17. Hollingsworth SA, Dror RO. Molecular dynamics simulation for all. Neuron. 2018;99(6):1129–43.
18. Haq FU, Abro A, Raza S, Liedl KR, Azam SS. Molecular dynamics simulation studies of novel β-lactamase inhibitor. J Mol Graph Model. 2017;74:143–52.
19. De Vivo M, Masetti M, Bottegoni G, Cavalli A. Role of molecular dynamics and related methods in drug discovery. J Med Chem. 2016;59(9):4035–61.
20. Azzam KM Al. SwissADME and pkCSM webservers predictors: an integrated online platform for accurate and comprehensive predictions for in silico ADME/T properties of artemisinin and its derivatives. Kompleks Ispolz Miner Syra. 2023;325(2):14–21.
21. Ferreira LLG, Andricopulo AD. ADMET modeling approaches in drug discovery. Vol. 24, Drug Discovery Today. 2019. p. 1157–65.